Contents list available at IJRED website

International Journal of Renewable Energy Development

Journal homepage: https://ijred.undip.ac.id

Research Article

An Effect of Wind Veer on Wind Turbine Performance

Undarmaa Tumenbayar[a] and Kyungnam Ko[b*]

[a] *Multidisciplinary Graduate School Program for Wind Energy, Jeju National University, 102 Jejudaehakro, Jeju, 63243, South Korea*

[b] *Department of Electrical and Energy Engineering, Jeju National University, 102 Jejudaehakro, Jeju, 63243, South Korea*

Abstract. An investigation was performed to identify the wind veer impact on wind turbine power performance at a wind farm located on Jeju Island, South Korea. A 2 MW wind turbine was used as a test turbine. An 80 m-tall met mast was located 220 m away from the test wind turbine and a ground lidar was installed close to the met mast. The wind veer conditions were divided into four types: veering in upper and lower rotor (VV), veering in upper and backing in lower rotor (VB), backing in upper and lower rotor (BB) and backing in upper and veering in lower rotor (BV). The frequency of the four types was identified at the wind farm. The characteristics of wind veer was analysed in terms of diurnal variation and wind speed. In addition, the power curves of the four types were compared with that under no veer condition. Also, the power deviation coefficient (PDC) derived from the power outputs was calculated to identify the effect of the four types on the turbine power performance. As a result, the frequencies of the types, VV, VB, BB and BV were 62.7 %, 4.9 %, 9.2 % and 23.1 %, respectively. The PDCs for the types VV and BV were 3.0 % and 4.2 %, respectively, meaning a power gain while those for the types VB and BB were -2.9 % and -3.9 %, respectively, meaning a power loss.

Keywords: Wind data, Ground lidar, Wind veer, Power curve, Power performance

Received: 27th July 2022; Revised: 22nd Sept 2022; Accepted: 25th Oct 2022; Available online: 8th Nov 2022

1. Introduction

The term, wind veer refers to the variation of the wind direction with height which is mainly caused by the friction and the pressure gradient as well as the balance on the Coriolis force. Wind veer can be categorized as veering wind and backing wind regarding the wind direction change with height. In the northern hemisphere of the earth, the veering wind which shifts clockwise with height is primarily associated with warm air advection. On the other hand, the backing wind which shifts counter clockwise with height, is usually related to the cold air advection (Ansorge and Wurps, 2022; Eriksson *et al.,* 2019; Shu *et al.,* 2020a).

There have been wind veer studies, which can be categorized as follows: wind veer characteristics (Abkar *et al.,* 2018; Bodini *et al.*, 2019; Brugger *et al.*, 2020; Churchfield and Sirnivas, 2018; Shu *et al.*, 2020b), its impacts on turbine power production (Englberger *et al.*, 2020; Gao *et al.,* 2021; Murphy *et al.*, 2020; Sanchez Gomez and Lundquist, 2020a, 2020b; Wagner *et al.*, 2010) and turbine wake deflection (Brugger *et al.*, 2019; Englberger and Lundquist, 2020; Gadde and Stevens, 2019; Howland and Dabiri, 2020; Lundquist, 2022; Narasimhan *et al.,* 2021).

The wind veer characteristics can vary with diurnal or seasonal conditions. Shu et al. (Shu et al., 2020b) performed a study on seasonal and diurnal variations of wind characteristics using lidar measurement data over the span of 4 years. The results showed a higher value of wind veer appearing during the night-time compared to the daytime. Similar trends were also obtained by Abkar *et al.* (Abkar *et al.*, 2018) using large-eddy simulations (LESs) combined with the actuator-disk model for a turbine rotor. It was reported that wind veer was more substantial during the nocturnal time associated with a stable atmosphere, while weaker wind veer tended to occur during diurnal time with convective flows.

Modern large wind turbines could experience considerable wind veer across large turbine rotors under specific conditions. In these cases, the wind direction at the hub height of the turbine does not represent the wind direction across the rotor, which may affect the wake behind the turbines. The characteristics of wind turbine wakes were revealed more accurately when wind veer was taken into consideration (Brugger *et al.*, 2019). It was pointed out that the magnitude of inflow wind veer toward a wind turbine decreased after passing through the turbine rotor resulting in less wake veer and a change of the wind veer in shape (Englberger and Lundquist, 2020).

Several studies have been conducted to investigate the wind veer effects on wind turbine power performance. Wagner et al. (Wagner *et al.*, 2010) carried out the simulation of wind veer impact on wind turbine power performance. It was found that a small clockwise wind veer brought an increase to the performance of a wind turbine, while a counter clockwise wind veer always caused a decrease of the power performance. Sanchez Gomez and Lundquist (Sanchez Gomez and Lundquist, 2020b) pointed out that the larger wind veer value was found in the morning compared to the evening. The bigger wind veer value combined with the small wind shear exponent, **α**, led to wind turbine underperformance, while overperformance

* Corresponding author
Email: gnkor2@jejunu.ac.kr (Kyungnam Ko)

https://doi.org/10.14710/ijred.2023.47905
ISSN: 2252-4940/© 2023.The Author(s). Published by CBIORE

appeared under the condition of a smaller wind veer value with a large wind shear exponent.

They also reported that a large veering wind resulted in greater wind turbine underperformance than a small backing wind, while a small veering wind led to overperformance of the turbine (Sanchez Gomez and Lundquist, 2020a). Murphy et al. (Murphy *et al.*, 2020) experimentally showed that the backing wind caused about a 0.7% less power production while the veering wind led to about a 1.3% greater power production.

However, a phenomenon of wind veer has been investigated mainly dividing into two types: veering wind and backing wind. It is necessary to consider various types of wind veer since the atmosphere, where a wind turbine operates, varies with various conditions such as terrain, surrounding roughness and obstacles as well as atmospheric stability conditions.

The purpose of this work is to reveal the effect of four types of wind veer on wind turbine power performance. The four types were defined in accordance with wind directions at upper blade tip, hub and lower blade tip heights. The power curves considering the four types were compared with that under no veering condition for identifying the power deviation.

2. Test setup and methodology

2.1 Test site

This work was performed at a real wind farm on Jeju Island which is located off the southern part of the Korean peninsula. Fig. 1 represents the location of Jeju Island and the layout around the test wind turbine of the wind farm. The wind farm has 15 wind turbines of 2 MW and is situated in the north-eastern part of the island. Turbine no. 15 was used as a test wind turbine for this study. A met mast and a ground lidar were used for measuring wind conditions. There is a landfill located close to the wind farm. The measurement sector is calculated by the following equation (International Electrotechnical Commission, 2022a):

$$\theta = 1.3arctan(2.5D/L + 0.15) + 10 \qquad (1)$$

where, D is the rotor diameter and L is the distance between wind turbines. The measurement sector was from 273° to 93° at this test setup.

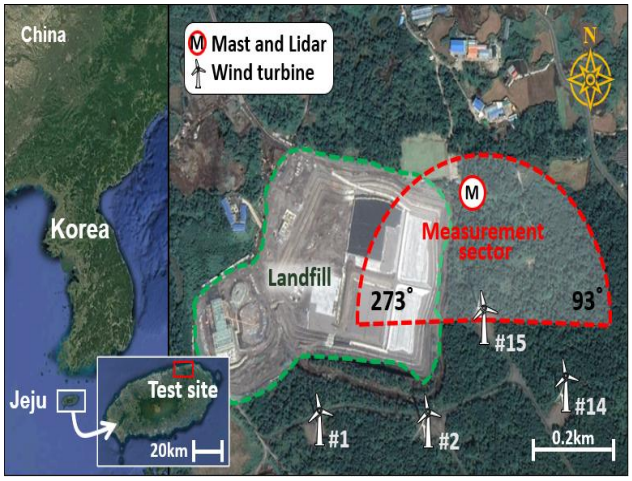

Fig. 1 Location of Jeju Island and layout of the measurement instruments and test wind turbine at the test wind farm

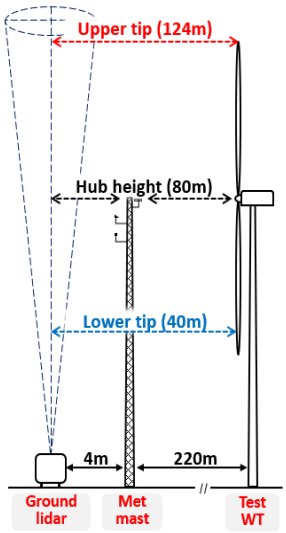

Fig. 2 Test wind turbine and measurement instruments

2.2 Test instruments

Fig. 2 shows the test wind turbine and the measurement instruments. An 80m-tall met mast was installed 220 m away from the test wind turbine and a ground lidar was installed 4 m from the met mast. The wind conditions across the rotor were measured by the sensors on the met mast and laser beams emitted from the ground lidar. The 10-minute averaged wind measurements were analysed with power production data of the test wind turbine. The measurements were collected for about 6 months from the 2nd of October, 2018, to the 19th of April, 2019. Table 1 shows the specification of the measurement instruments and the test wind turbine. Wind speed and direction at hub height were measured by the Thies first class anemometer and the wind vane.

Table 1
Specification of the measurement instruments and test wind turbine

Category		Specification
Met mast	Cup anemometer	Thies first class advanced
	Wind vane	Thies first class advanced
	Thermometer	PT 100 CLA
	Hygrometer	Portronics hygrometer
	Barometer	P-GE 6/11
Ground lidar	Model	Windcube V2
	Measurement range	40~200 m
	Sampling rate	1 Hz
	No. of measurement	12
	Analysed measurement points	40, 80, 124 m
Wind turbine	Model	HJWT 2000
	Rated power	2000 kW
	Hub height	80 m
	Rotor diameter	87 m
	Cut-in wind speed	3 m/s
	Rated wind speed	12 m/s
	Cut-out wind speed	25 m/s
	SCADA system	Gateway

The air temperature, the humidity and atmospheric pressure were used for normalization of the specific air density at the test site which were measured at a height of 75 m by the meteorological sensors listed in Table 1. The ground lidar used was the Windcube v2 developed by Leosphere. It has five laser beams that are emitted vertically to measure wind conditions at 12 points from 40 to 200 m over the ground level. The 2 MW wind turbine was tested for this investigation, whose hub height and rotor diameter were 80 and 87 m, respectively. The power outputs from the test wind turbine were collected through the Gateway Supervisory control and data acquisition (SCADA) system.

2.3 Data filtering

The measured raw data from the ground lidar was filtered according to the study by Shin *et al.* (Shin and Ko, 2019) and the ground lidar user manual (Leosphere, 2014). The filtering criteria of the wind measurements are listed below:

- Data outside of the measurement sector
- Data with lidar availability less than 80%
- Data with a carrier to noise ratio less than -23 dB
- Data measured by lidar in abnormal operation

The data recorded with the conditions above were discarded for the analysis.

Additionally, when wind turbine was producing electrical power significantly lower or higher than the expected power, and the wind turbine was in abnormal operation, or when the yaw misalignment was over 30° (Sereema, 2020), the wind measurements and the power data were removed from the database. Also, the wind speeds lower than the cut-in and higher than the cut-out speeds were discarded for the analysis.

After the filtering process, the data recovery rate was approximately 50.7%, which is named as all data for formal analysis.

2.4 Methodology

First, the wind speeds and directions measured from the reference met mast and the lidar device were compared for verification of the lidar measurements.

Then, the measured power curves were determined according to the IEC 61400-12-1 3rd edition standards (International Electrotechnical Commission, 2022b). To estimate the power curve, the measured wind speeds were normalized to standard air density by the following equation:

$$V_n = V_{10min}\left(\frac{\rho_{10min}}{\rho_0}\right)^{\frac{1}{3}} \quad (2)$$

where, V_n is normalized wind speed, V_{10min} is 10-minute averaged wind speed, ρ_{10min} is 10-minute averaged air density, and ρ_0 is the reference air density.

The measured power curve under no veer condition was drawn using hub height wind speeds and power outputs with wind veer within ±0.01˚/m (Gao *et al.,* 2021). The wind data under no veer condition accounted for 11.3% of all data.

The degree of wind veer per meter, γ, was analysed between 40 m and 124 m across the rotor by the following equation:

$$\gamma = \frac{\theta_U - \theta_L}{Z_U - Z_L} \quad (3)$$

where, θ_U and θ_L are wind directions at rotor upper and lower measurement points and Z_U and Z_L are heights of rotor upper and lower measurement points, respectively.

Since a phenomenon of wind veer was related to the atmospheric stability condition (Gao *et al.*, 2021), the bulk Richardson number, Ri_b, was utilized at the site for analysing the stability condition. Ri_b is expressed as the following equation (Bahamonde and Litrán, 2019):

$$Ri_b = \frac{gz(T_1 - T_2)}{(273.15 + T_1)V^2} \quad (4)$$

where, g is the acceleration due to gravity, V is the wind speed measured at height z and T_1 and T_2 were the air temperatures at 75 m and 3 m in this study, respectively.

Lastly, the power deviation coefficient (PDC) was calculated by the following equation:

$$PDC = \frac{\sum P_{four\ types} - \sum P_{no\ veer}}{\sum P_{no\ veer}} \times 100\% \quad (5)$$

where, $P_{four\ types}$ and $P_{no\ veer}$ are power outputs of the four types and no veer condition, respectively. The negative and positive values of PDC indicate power loss and power gain, respectively. The PDC for each type was analysed using power outputs before the rated wind speed in this work.

3. Result and discussion

3.1 Fundamental analysis

The wind speed and the direction data at 80 m height from the met mast and the ground lidar were compared to check for correlation.

Fig. 3 presents the result of the linear regression analysis between the ground lidar and the met mast wind speeds. The correlation was very high with a linear line slope of 0.9955 and a coefficient of determination, R^2, of 0.9958. Fig. 4 shows the wind roses of the met mast and the ground lidar wind directions. The two wind roses were very similar to each other and the prevailing wind direction was from the northwest.

Fig. 5 represents the measured power curves using all data points and no veer data points. The measured power curve using all data points was higher than that using no veer data points. The measured power curve using no veer data points was used as the reference power curve for this work.

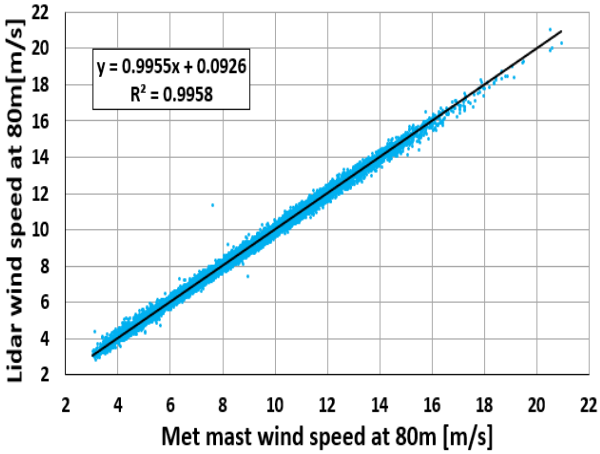

Fig. 3 Linear regression analysis between met mast and ground lidar wind speeds

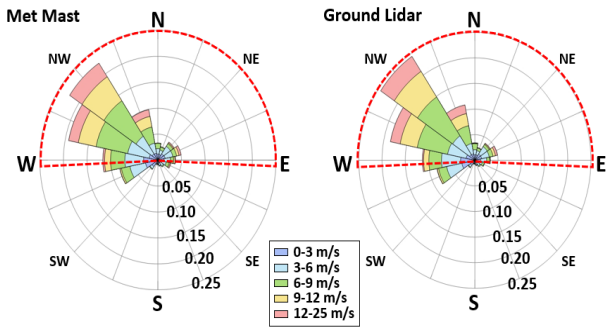

Fig. 4 Wind roses of met mast and ground lidar wind directions. The red dotted lines highlight the measurement sector

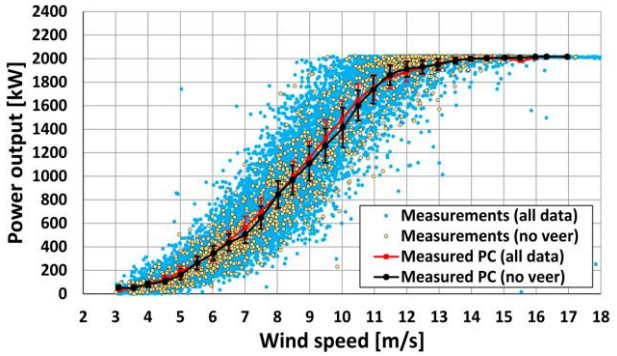

Fig. 5 Measured power curve using all data points and under no veer condition. The error bar corresponds to one standard deviation.

3.2 Wind veer characterization

Fig. 6 presents the frequency of wind veer. It shows 83.1 % for veering wind that changes directions in clockwise rotation with height, and 16.9 % for backing wind which changes directions in counter clockwise rotation with height. The mean wind veer during the measurement period was 0.05 deg./m due to the higher occurrence of veering winds. Such dominant veering winds could be associated with relatively higher stable and neutral atmospheric conditions at the site (Abkar *et al.*, 2018), where the conditions during the measurement period were 35.0 %, 41.5 % and 23.5 % for stable, neutral and unstable conditions, respectively.

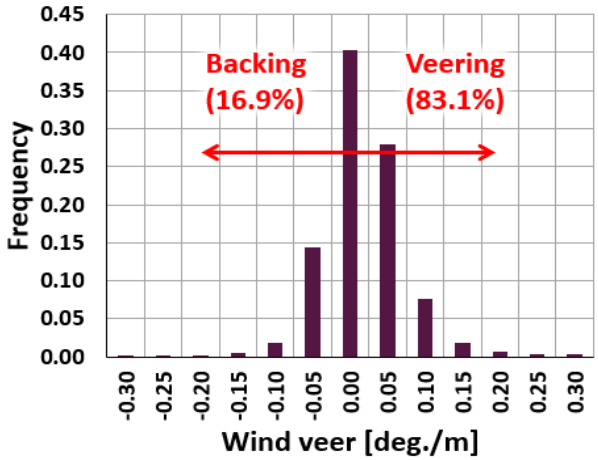

Fig. 6 Frequency of wind veer using all data points.

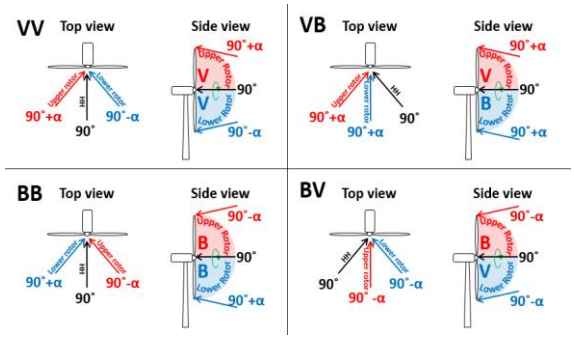

Fig. 7 Schematic illustration of wind veer types. α is the degree of wind direction change.

The variation of the wind veer across the rotor may affect the forces and loads on wind turbine blades. To investigate more accurate effects of wind veer, wind veer was divided into four types for this study based on the wind direction change from an upper measurement point to hub height and hub height to a lower measurement point (Gao *et al.*, 2021). Fig. 7 shows four types of wind veer conditions in the case of incoming wind from the east of 90°. Those are veering in upper rotor and also veering in lower rotor (VV), veering in upper rotor and backing in lower rotor (VB), backing in upper rotor and also backing in lower rotor (BB) and backing in upper rotor and veering in lower rotor (BV). The turbine yaw misalignment was not taken into consideration in this study.

The frequency of the four types of wind veer is listed in Table 2. The types VV, VB, BB and BV occupied 62.7%, 4.9%, 9.2% and 23.1% of all data points, respectively. Type VV had only positive wind veer values that concentrated between 0.03 to 0.13 deg./m, while type BB showed only negative wind veer values of which the median -0.05 deg./m had the most frequency. The positive and the negative wind veer values could be found at types VB and BV. Type VB appeared mostly between -0.03 to 0.03 deg./m, while type BV had the highest frequency in the range of -0.03 to 0.08 deg./m. Due to the combination of veering and backing winds across the rotor diameter, the frequencies of the types VB and BV concentrated on zero deg./m.

Table 2
Frequency of the four types of wind veer

Median [deg./m]	Range [deg./m]		VV	VB	BB	BV
-0.30	-0.32	-0.27	0.0%	0.0%	0.1%	0.0%
-0.25	-0.27	-0.22	0.0%	0.0%	0.2%	0.0%
-0.20	-0.22	-0.17	0.0%	0.0%	0.2%	0.0%
-0.15	-0.17	-0.12	0.0%	0.0%	0.3%	0.0%
-0.10	-0.12	-0.07	0.0%	0.0%	0.8%	0.0%
-0.05	-0.07	-0.02	0.0%	0.4%	3.9%	0.6%
0.00	-0.03	0.03	7.1%	4.4%	3.6%	12.7%
0.05	0.03	0.08	31.7%	0.2%	0.0%	8.6%
0.10	0.08	0.13	15.6%	0.0%	0.0%	1.1%
0.15	0.13	0.18	4.0%	0.0%	0.0%	0.1%
0.20	0.18	0.23	1.1%	0.0%	0.0%	0.0%
0.25	0.23	0.28	0.5%	0.0%	0.0%	0.0%
0.30	0.28	0.33	0.3%	0.0%	0.0%	0.0%
Sum*			60.4%	4.9%	9.1%	23.1%
Total**			62.7%	4.9%	9.2%	23.1%

* Summation of the presented frequency
** Total frequency considering the all data

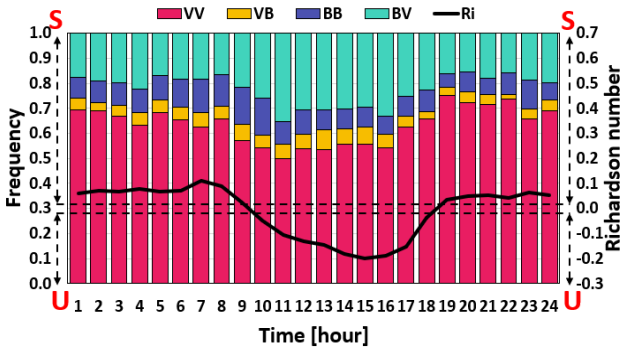

Fig. 8 Average diurnal variation of wind veer frequency according to the four types with diurnal atmospheric stability analysis. U and S represent unstable and stable conditions.

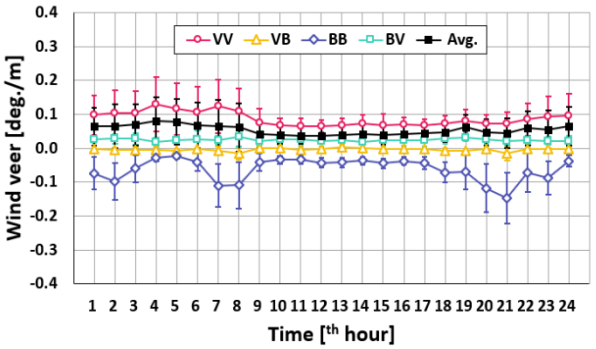

Fig. 10 Diurnal variation of wind veer according to the four types. The error bar corresponds to one standard deviation.

Fig. 8 shows diurnal frequency variation of the four types including the variation of atmospheric stability condition. The types VV and BV had opposing trends with each other throughout the whole day. Type VV displayed a higher frequency during the nighttime when atmospheric conditions were mainly stable, while type BV showed more occurrence during the daytime when unstable conditions were prevailing. The remaining two types roughly had the same variation throughout the whole day.

Fig. 9 illustrates diurnal variation of the hub height wind speed. The lower wind speeds occurred during the daytime while the higher wind speed occurred during the night-time. The average wind speed was 8.17 m/s during the analysed period. The standard deviation rarely varied with hours, of which the average value was 1.46 m/s.

The hourly mean wind veer for the four types, including the average value, is shown in Fig.10. The average values were higher with bigger standard deviations during the night-time compared to the daytime. The wind veer for VV and BB increased and fluctuated more during the night-time than the daytime. Type VV had almost the same trend as the average values of the wind veer since it took 62.7 % of the total data points. Type VB had mostly negative wind veers whose average was -0.004 deg./m, while type BV had all positive values with an average of 0.024 deg./m. Types VB and BV presented very little diurnal and hourly variations.

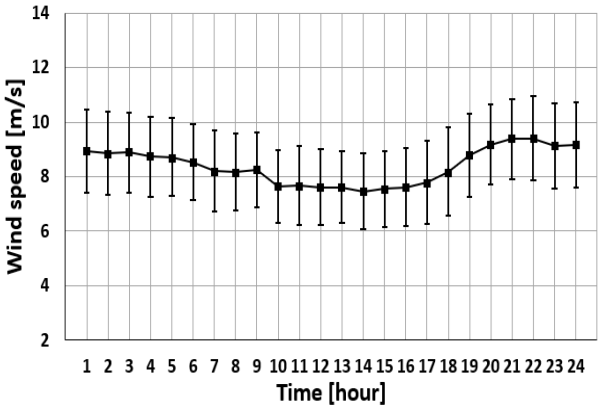

Fig. 9 Diurnal variation of hub height wind speed. The error bar corresponds to one standard deviation.

Fig.11 displays the mean wind veer variation with wind speeds for the four types including the average value. As the wind speed increased, the values of the wind veer decreased. The fluctuation of the wind veer at lower wind speeds was greater than that at higher wind speeds. Highest wind veer and variation were found with a decrease of wind speed for type VV. The same trends as these findings were reported by Kawabata and Kogaki. (Kawabata and Kogaki, 2020). Murphy et al. also found that the small wind shear and small wind veer resulted from high wind speeds that mechanically mix momentum at all measurement heights (Murphy *et al.*, 2020).

3.3 Power output

Fig. 12 represents the power curves under no wind veer condition as well as the four types. The power output difference is the power outputs of the four types minus those of no veer condition. The power output fluctuations before the rated wind speed were greater than those after the rated speed. The power outputs before the rated wind speed for types VV and BV were mostly higher than those under the no veer condition, while those for types VB and BB had almost all lower values than those under the no veer condition. Similar results were found by Murphy *et al.* (Murphy *et al.*, 2020).

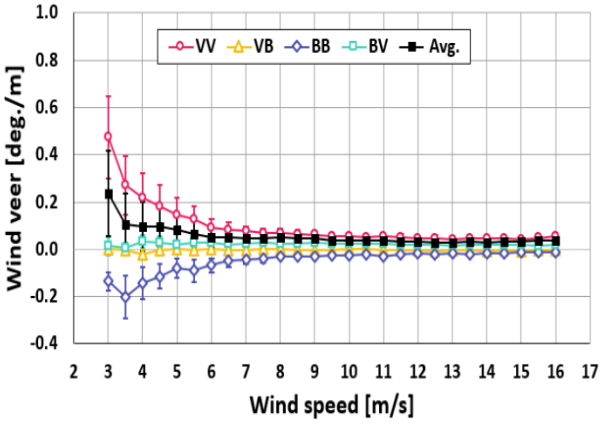

Fig. 11 Mean wind veer variation according to wind speed for each case. The error bar corresponds to one standard deviation.

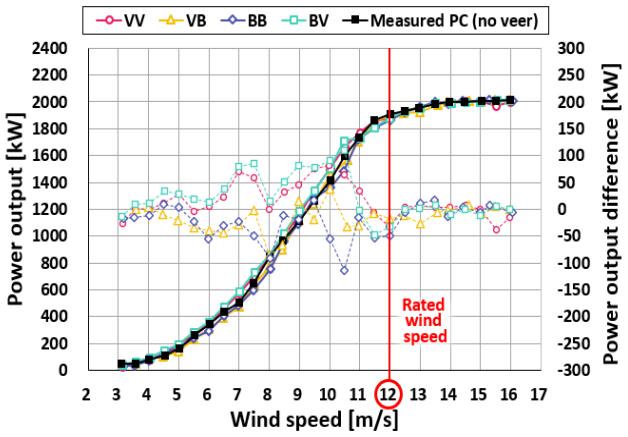

Fig. 12 Power curve and power output difference according to the four types

Table 3
Average wind veer and PDC for four types

Type	Wind veer		PDC [%]	Note
	Value [deg./m]	Profile		
VV	0.092	Veering	3.0%	Gain
VB	-0.003	Backing	-2.9%	Loss
BB	-0.066	Backing	-3.9%	Loss
BV	0.025	Veering	4.2%	Gain

Table 3 represents the average wind veers and PDC according to the four types. Types VV and BV had the positive values of 0.092 and 0.025 deg./m, respectively, which defines the veering wind, while types VB and BB had the negative values of -0.003 and -0.066 deg./m, respectively, which is the backing wind. The PDCs of types VV and BV were 3.0 % and 4.2 %, respectively, which represents a power gain, while those of types VB and BB were -2.9 % and -3.9 %, respectively, which were a power loss. This result was in good agreement with the simulation result conducted by Wagner *et al.* (Wagner *et al.,* 2010).

4. Conclusions

In this study, an experimental work was carried out to investigate the characteristics of wind veer and its impact on wind turbine power performance. The wind veer types, VV, VB, BB and BV were found 62.7 %, 4.9 %, 9.2 % and 23.1 % of the qualified data points, respectively. Type VV occurred more frequently during the night-time with stable atmospheric conditions, while type BV occurred more during the daytime with unstable conditions. As the wind speed increased, the wind veers had lower values and fluctuations. Lastly, the PDCs of types VV and BV were 3.0 % and 4.2 %, respectively, representing a power gain. On the other hand, types VB and BB had the PDCs of -2.9 % and -3.9 %, respectively, meaning a power loss.

Acknowledgments

This research was supported by the 2021 Scientific Promotion Program funded by Jeju National University.

Author Contributions: UT.: Conceptualization, Methodology, Software, Formal analysis, Investigation, Writing - original draft, Visualization. KK.: Writing - review & editing, Supervision, Project administration. All authors have read and agreed to the published version of the manuscript.

Conflicts of Interest: The authors declare no conflict of interest.

References

Abkar, M., Sørensen, J.N., Porté-Agel, F., (2018). An analytical model for the effect of vertical wind veer on wind turbine wakes. *Energies* 11, 1838. https://doi.org/10.3390/en11071838

Ansorge, C., Wurps, H., (2022). Wind veer and wind speed in turbulent Ekman flow. Copernicus Meetings. https://doi.org/10.1088/1742-6596/1256/1/012026

Bahamonde, M.I., Litrán, S.P., (2019). Study of the energy production of a wind turbine in the open sea considering the continuous variations of the atmospheric stability and the sea surface roughness. *Renewable Energy* 135, 163–175. https://doi.org/10.1016/j.renene.2018.11.075

Bodini, N., Lundquist, J.K., Kirincich, A., (2019). US East Coast lidar measurements show offshore wind turbines will encounter very low atmospheric turbulence. *Geophysical Research Letters* 46, 5582–5591. https://doi.org/10.1029/2019GL082636

Brugger, P., Debnath, M., Scholbrock, A., Fleming, P., Moriarty, P., Simley, E., Jager, D., Roadman, J., Murphy, M., Zong, H., (2020). Lidar measurements of yawed-wind-turbine wakes: characterization and validation of analytical models. *Wind Energy Science* 5, 1253–1272. https://doi.org/10.5194/wes-5-1253-2020

Brugger, P., Fuertes, F.C., Vahidzadeh, M., Markfort, C.D., Porté-Agel, F., (2019). Characterization of wind turbine wakes with Nacelle-Mounted Doppler LiDARs and model validation in the presence of wind veer. *Remote Sensing* 11, 2247. https://doi.org/10.3390/rs11192247

Churchfield, M.J., Sirnivas, S., (2018). On the effects of wind turbine wake skew caused by wind veer, in: 2018 Wind Energy Symposium. p. 755. https://doi.org/10.2514/6.2018-0755

Englberger, A., Lundquist, J.K., (2020). How does inflow veer affect the veer of a wind-turbine wake?, *Journal of Physics*: Conference Series. IOP Publishing, p. 12068. https://doi.org/10.1088/1742-6596/1452/1/012068

Englberger, A., Lundquist, J.K., Dörnbrack, A., (2020). Should wind turbines rotate in the opposite direction? *Wind Energy Science*, 1–20. https://doi.org/10.5194/wes-2019-105

Eriksson, O., Breton, S.-P., Nilsson, K., Ivanell, S., (2019). Impact of wind veer and the Coriolis force for an idealized farm to farm interaction case. *Applied Sciences* 9, 922. https://doi.org/10.3390/app9050922

Gadde, S.N., Stevens, R.J.A.M., (2019). Effect of Coriolis force on a wind farm wake, in: *Journal of Physics: Conference Series*. IOP Publishing, p. 12026. https://doi.org/10.1088/1742-6596/1256/1/012026

Gao, L., Li, B., Hong, J., (2021). Effect of wind veer on wind turbine power generation. *Physics of Fluids* 33, 15101. https://doi.org/10.1063/5.0033826

Howland, M., Dabiri, J., (2020). Influence of atmospheric boundary layer wind speed and direction shear on utility-scale yaw misaligned turbines, in: APS Division of Fluid Dynamics Meeting Abstracts. pp. G03-004. https://doi.org/10.1063/5.0023746

International Electrotechnical Commission, (2022a). Wind energy generation systems Part 12-5: Power performance – Assessment of obstacles and terrain, International Electrotechnical Commission.

International Electrotechnical Commission, (2022b). Wind energy generation systems Part 12-1: Power performance measurements of electricity producing wind turbines, International Electrotechnical Commission.

Kawabata, H., Kogaki, T., (2020). Lidar-assisted yaw control for wind turbines using a 9-beam nacelle lidar demonstrator, in: *Journal of Physics: Conference Series*. IOP Publishing, p. 12056. https://doi.org/10.1088/1742-6596/1452/1/012056

Leosphere, (2014). Windcube V2 liDAR Remote Sensor User Manual.

Lundquist, J.K., (2022). Wind Shear and Wind Veer Effects on Wind

Turbines, in: Handbook of Wind Energy Aerodynamics. Springer, pp. 1–22. https://doi.org/10.1007/978-3-030-05455-7_44-1

Murphy, P., Lundquist, J.K., Fleming, P., (2020). How wind speed shear and directional veer affect the power production of a megawatt-scale operational wind turbine. *Wind Energy Science* 5, 1169–1190. https://doi.org/10.5194/wes-5-1169-2020

Narasimhan, G., Gayme, D., Meneveau, C., (2021). Effect of veer on a yawed wind turbine wake in neutral and stable atmospheric boundary layer, in: APS Division of Fluid Dynamics Meeting Abstracts. pp. H03-007.

Sanchez Gomez, M., Lundquist, J.K., (2020a). The effect of wind direction shear on turbine performance in a wind farm in central Iowa. *Wind Energy Science* 5, 125–139. https://doi.org/10.5194/wes-5-125-2020

Sanchez Gomez, M., Lundquist, J.K., (2020b). The Effects of Wind Veer During the Morning and Evening Transitions. J*ournal of Physics: Conference Series*. IOP Publishing, p. 12075. https://doi.org/10.1088/1742-6596/1452/1/012075

Sereema, (2020). Wind Turbine Yaw Misalignment: (R)Evolution.

Shin, D., Ko, K., (2019). Application of the nacelle transfer function by a nacelle-mounted light detection and ranging system to wind turbine power performance measurement. *Energies* 12, 1087. https://doi.org/10.3390/en12061087

Shu, Z., Li, Q., He, Y., Chan, P.W., (2020a). Investigation of marine wind veer characteristics using wind lidar measurements. *Atmosphere* 11, 1178. https://doi.org/10.3390/atmos11111178

Shu, Z., Li, Q.S., Chan, P.W., He, Y.C., (2020b). Seasonal and diurnal variation of marine wind characteristics based on lidar measurements. *Meteorological Applications* 27, e1918. https://doi.org/10.1002/met.1918

Wagner, R., Courtney, M., Larsen, T.J., Paulsen, U.S., (2010). Simulation of shear and turbulence impact on wind turbine performance. Danmarks Tekniske Universitet, Risø Nationallaboratoriet for Bæredygtig Energi.